November 19, 1996 BNL-63842
CONF-9609315--1

Structures and Incommensurate Spin Excitations in Excess Oxygen-Doped La_2CuO_{4+y}

R. J. Birgeneau[1)], R. J. Christianson[1)], Y. Endoh[2)], M. A. Kastner[1)], Y. S. Lee[1)], G. Shirane[3)], B. O. Wells[1)], K. Yamada[2)]

[1)] *Department of Physics, Massachusetts Institute of Technology, Cambridge, MA, 02139, USA*

[2)] *Department of Physics, Tohoku University, Aramaki Aoba, Sendai, 980-77, Japan*

[3)] *Department of Physics, Brookhaven National Laboratory, Upton, NY 11973, USA*

Abstract

Over the past decade, we have studied in detail the low energy spin fluctuations in $La_{2-x}Sr_xCuO_4$ for x between 0 and 0.18. Our experiments, as well as those by others, have revealed a fascinating interplay between the hole doping, the static and dynamic spin fluctuations and the superconductivity. Recently, using electrochemical techniques, we have learned how to produce large single crystals of La_2CuO_{4+y} which are relatively homogenous. In this latter system, the dopants are characterized by annealed rather than quenched disorder. Furthermore, we have demonstrated staging behavior of the excess oxygen analogous to staging in intercalated graphite. We have now succeeded in carrying out measurements of the low energy spin fluctuations in stage-6 La_2CuO_{4+y}. Specifically, we find that in this system which has $T_c = 31$ K, the spin fluctuations are incommensurate with energy and temperature dependencies very much like those in $La_{1.85}Sr_{0.15}CuO_4$ with $T_c = 33$ K. In addition, we find that T_c/δ is a constant for high quality materials in both $La_{2-x}Sr_xCuO_4$ and La_2CuO_{4+y}, here δ is the incommensurability.

Keywords: Superconductivity, Magnetism, Staging

Robert J. Birgeneau, Rm. 6-123, MIT, Cambridge, Ma 02139

Fax: (617) 253-8901, Email: robertjb@mit.edu

I. INTRODUCTION

After a decade of intensive research, it has become clear that the phenomenon of high temperature superconductivity is characterized by both great complexity and rich physics. Much of the materials effort in this field has been focused on producing materials with higher transition temperatures. Our efforts, instead, have been centered on producing materials which will allow insight into the basic physics of the overall copper oxide phases and phase diagram including the superconductors. Toward this end we are interested in finding simple materials which allow for illustrative experiments. As part of this approach, we have pursued an extensive project on the La_2CuO_{4+y} system [1,2]. As we will discuss below, this material has an elaborate series of structural phases. Recently, we have performed inelastic magnetic neutron scattering studies of superconducting $La_2CuO_{4.055}$ [2]. Of particular importance is the comparison of the magnetic excitations in the La_2CuO_{4+y} compound with those in $La_{2-x}Sr_xCuO_4$ [3]. Both materials are based upon the original parent compound La_2CuO_4, but the nature of the dopant ions and the structures are fundamentally different in the two compounds. The Sr^{++} dopants in $La_{2-x}Sr_xCuO_4$ enter the structure substitutionally for La ions while the oxygen dopants in La_2CuO_{4+y} occupy interstitial sites [4,5]. The Sr^{++} ions are essentially immobile once the crystal solidifies below $\sim$1400 K, while the excess oxygen dopants in La_2CuO_{4+y} remain mobile down to near 200 K. Thus a comparison of the two systems allows us to test the influence of quenched versus annealed disorder upon the properties of a given high-T_c system.

The format of this paper is as follows. In Section II we review the phase diagram and structures of La_2CuO_{4+y}. Section III contains a review of the recent magnetic inelastic neutron scattering measurements in $La_2CuO_{4.055}$ [2]. A discussion is given in Section IV.

II. PHASE DIAGRAM AND STRUCTURES

The phase diagram which we have determined for excess oxygen La_2CuO_4 is shown in the bottom panel of Fig. 1. Comparison with the corresponding phase diagram of $La_{2-x}Sr_xCuO_4$ [6], displayed in the top panel, shows that the two systems exhibit fundamentally different behaviors. The reason for this, as noted above, is that the Sr^{++} ions are totally frozen below the growth temperature, whereas the O^{--} intercalant ions are mobile down to ~200 K [1,2,4,5]. Thus, except for concentrations corresponding to near-integer staging as described below, the O^{--} ions phase separate into regions of smaller and larger O^{--} concentrations. The phase separation between $y \simeq 0.01$ and $y \simeq 0.055$ shown in Fig. 1 had been extensively explored by Johnston and co-workers prior to our work [4,5].

As a result of a concerted materials effort, we have learned how to grow and electrochemically intercalate large, narrow mosaic single crystals of La_2CuO_{4+y} with y up to ~ 0.1 and volumes approaching 1 cc. This has enabled us to elucidate the basic structures of the materials. Further, these single crystals make possible studies of the lattice and spin excitations in the superconducting concentration range. We have found that the low temperature structure of La_2CuO_{4+y} for $y \geq 0.055$ is orthorhombic with a superlattice structure along the c axis [1]. The diffraction is consistent with a structural model originally proposed for $La_2NiO_{4+\delta}$ [7]. In this model, the CuO_6 octahedra are tilted. Within the planes, the tilts are ordered in the same manner as in undoped La_2CuO_4 and perpendicular to the planes the tilts have the same local ordering. The structure of La_2CuO_{4+y} with $y \geq 0.055$ differs from that of La_2CuO_4 in that the doped material contains broad antiphase domain boundaries regularly spaced along the c axis, perpendicular to the CuO_2 planes. The antiphase domain boundaries consist of layers across which the direction of the CuO_6 tilts are reversed. Within this model the antiphase domain boundaries are presumed to be caused by ordered layers of interstitial oxygen. This one-dimensional ordering of the extra oxygen is similar to the staging behavior of halogens and alkalis intercalated into graphite. Following the literature on intercalated graphite, we use the term "staging" to describe the c axis modulation of the un-

doped structure; stage n refers to an induced periodicity of n CuO_2 host layers. La_2CuO_{4+y} thus presents an interesting contrast with $La_{2-x}Sr_xCuO_4$ since the dopants which contribute the charge carriers give rise to annealed rather than quenched disorder.

For excess oxygen concentrations between ~0.01 and ~0.055, the behavior as a function of temperature is quite elaborate. Phase separation occurs below $T_{PS} \simeq 290$ K. The onset of stage ordering in the oxygen rich phase occurs at $T_{SO} \simeq 255$ K. The staging number evolves from ~7 to ~6 with decreasing temperature [1]. If the sample is cooled through the temperature region around 210 K over a period of several hours, as recently reported by X. Xiong *et al.* [8], an additional phase transition occurs. This transition corresponds to the establishment of a mass density modulation along a with a periodicity of about 11.5 a [1]. T_c in the modulated phase is about 1.5 K higher than that in the quenched samples [8]. Increasing y beyond 0.055 results in samples with, in succession, stage n = 4,3,2. The exact oxygen concentration y for each of these stages is not yet known, nor is T_c, although preliminary evidence suggests $T_c(n = 2)$ may be as high as 45 K.

Clearly, the La_2CuO_{4+y} system represents a rich system for study of the structural, magnetic, transport, and superconducting properties. Most importantly, since the O^{--} intercalant ions are mobile at 200 K, which in energy units is much smaller than the important electronic and magnetic energies, the disorder in La_2CuO_{4+y} is annealed rather than quenched. Thus, by making detailed comparisons with the results in $La_{2-x}Sr_xCuO_4$, it should be possible to determine the relative effects of annealed versus quenched disorder on the normal state and superconducting properties.

III. SPIN EXCITATIONS

A great deal of effort has gone into studying the spin fluctuations in the high-T_c superconductors and related compounds [6,9,10]. In particular, understanding the magnetism of the undoped parent compounds has been one of the significant successes in the field [9,11]. While the superconductors themselves show no long range ordered magnetism of the Cu mo-

ments, there are clear short range antiferromagnetic correlations [9,10,12]. The mechanism of the disruption of the long range order by holes is still under debate.

The best and most extensive data exist for the $La_{2-x}Sr_xCuO_4$ system [9,10,12]. Neutron scattering studies have shown that antiferromagnetic spin fluctuations exist over a broad range of x [9]. For low doping values the peak positions, intensities, and correlation lengths show a simple evolution from the well understood undoped material, which exhibits 3D Néel order for $0 \leq x \leq 0.0175$. At higher doping $0.02 \leq x < 0.05$, the neutron scattering peaks indicate short range magnetic order with the characteristic antiferromagnetic wavevector $(\frac{1}{2}, \frac{1}{2})$ in reciprocal space for the two-dimensional square lattice [13]. However, in the doping regime where superconductivity appears, for $x \gtrsim 0.05$, the spin fluctuations no longer occur at $(\frac{1}{2}, \frac{1}{2})$ but split into four peaks located at $(\frac{1}{2} \pm \delta, \frac{1}{2})$ and $(\frac{1}{2}, \frac{1}{2} \pm \delta)$ as seen in Figure 2.

Neutron scattering experiments have also determined that for optimally doped $La_{2-x}Sr_xCuO_4$ in the superconducting state, the intensity of the spin fluctuations below 3.5 meV at $(\frac{1}{2} \pm \delta, \frac{1}{2})$ and $(\frac{1}{2}, \frac{1}{2} \pm \delta)$ are suppressed, vanishing as $T \rightarrow 0$ [3]. This suggests the formation of a superconducting magnetic gap. Indeed the observed magnetic gap is consistent with a $d_{x^2-y^2}$ superconducting order parameter with $2\Delta_o \simeq 6kT_c$ [3]. Earlier work on somewhat poorer quality underdoped samples showed that the low energy neutron scattering peaks are also suppressed at the above **q**-positions but the intensity does not go to zero at the lowest temperatures studied [9,10,14]. The energy range of the partial gap in these depressed T_c samples is similar to that where a complete gap is seen in the optimally doped sample. It is difficult to interpret the physical origin of this magnetic gap in the superconducting state without first understanding the origin of the magnetic peaks in the normal state.

There are many models which may account for the incommensurate splitting of the inelastic magnetic scattering peaks in $La_{2-x}Sr_xCuO_4$. Two of the most widely discussed are the nested Fermi surface model [15–17] and the charge fluctuation model. In the Emery and Kivelson version of the latter model [18] the doped holes segregate into one-dimensional

Cu-O chains or stripes which are non-magnetic and cause antiphase domain boundaries between the remaining undoped, antiferromagnetic regions. There is a great deal of ongoing research to try to determine if either of these two physical pictures or other proposed models is correct. Empirically, it must be determined whether the effect seen in $La_{2-x}Sr_xCuO_4$ is universal among different compounds with different types of dopants and how the effect develops as a function of doping. The experiments which we review here add to the empirical knowledge base in both of these areas.

Figure 2 shows a schematic of the trajectory for the scans we use to measure the incommensurate magnetic peaks. The original alignment of the crystal is such that the (H,0,L) zone is in the scattering plane. The scattering rods, which are at $(\frac{1}{2} \pm \delta, \frac{1}{2}, \mathrm{L})$ and $(\frac{1}{2}, \frac{1}{2} \pm \delta, \mathrm{L})$ in the square lattice notation appear at $(1 \mp \delta, \pm\delta, \mathrm{L})$ and $(1 \pm \delta, \mp\delta, \mathrm{L})$ in the Bmab notation. Thus, to scan over the incommensurate peaks we must scan outside of the (H,0,L) zone. This is accomplished by tilting the sample by 6° as shown in Figure 2. Since we are studying two-dimensional scattering rods, the value of L is immaterial except for purposes of maximizing the signal-to-background. We choose the L position to avoid anomalous background scattering and to optimize the instrumental focusing with the long axis of our scattering plane resolution ellipse lying along the rod. This configuration gives a better signal-to-background ratio than measurements of the same peaks in the (H,K,0) scattering zone [12,14].

Our inelastic magnetic scattering experiments on La_2CuO_{4+y} have been performed on two single crystal samples. Both have been intercalated with oxygen using electrolysis at 90° C in a D_2O solvent (in contrast to the H_2O solvent used in our previous studies [1]). We note that this substitution for solvents results in a subtle difference in the stage ordering temperature, possibly due to the intercalation of small quantitites of OD^- (versus OH^-). One sample (labeled Sendai-1 after the institution at which it was grown) has a mass of 3.366 grams and has an oxygen doping within the first miscibility gap region with approximately 80% of the sample on the oxygen rich side at low temperatures, about $O_{4.045}$, with a superconducting onset temperature of $T_c = 32$ K. The other sample (labeled MIT-1) weighs 1.927 grams with

an oxygen content just at the oxygen rich edge of the first miscibility gap, about $O_{4.055}$, with $T_c = 31$ K. These samples are less than one third the size of the crystals used for the best inelastic neutron scattering measurements on $La_{2-x}Sr_xCuO_4$. However they are about ten times larger than most of the crystals used in previous electrochemical oxygen intercalation studies.

The oxygen-rich portion of Sendai-1 has a staging number of 6.0 at low temperatures, while the oxygen-rich portion of MIT-1 is predominantly stage 6.2 with a small admixture of stage 4.1. Figure 3 shows longitudinal scans in **q** at an energy transfer of 2 meV for the Sendai-1 sample at different tilt angles. A tilt angle of 0° is equivalent to scanning along H in the (H,0,L) zone. We see two different sets of peaks in these scans. There is a peak at $(1, 0, L)$ seen most clearly in the 0° tilt scan, as well as peaks which are seen best in the 6° tilt scans at $(1 - \delta, \delta, \mathrm{L})$ and $(1 + \delta, \delta, \mathrm{L})$ where $\delta = 0.105$. The peak at (1,0,L) arises from spin waves in the oxygen-poor region of the crystal and those at $(1 \pm \delta, \delta, L)$ from spin excitations in the oxygen-rich region.

Our goal is to study the oxygen-rich material; thus the rest of the data we present comes from MIT-1, the sample near the high-y edge of the first miscibility gap. In this sample we see very little inelastic scattering at the (1,0,L) postion, indicating that only a small fraction of the sample consists of undoped CuO_2 planes. In Figure 4 we present the inelastic scattering peaks for an energy transfer of 2 meV at three representative temperatures $T =$ 50 K, 32 K ($\sim T_c$), and 11 K. The peak intensity appears to rise slightly from 50 K to 32 K but then is substantially reduced at 11 K. Similar behaviour is seen for our data taken at an energy transfer of 3 meV, but any such diminution of intensity for an energy transfer of 4 meV is very slight. This corresponds closely to the results by both the Brookhaven [12,14] and Risö [10] groups for $La_{2-x}Sr_xCuO_4$ samples with similar T_c.

In Figure 5 we present a summary plot of the imaginary part of the susceptibility $\chi''(\mathbf{q} = \mathbf{Q}_\delta, \omega)$ versus temperature at three small energy transfers for both this sample of La_2CuO_{4+y} and the $La_{2-x}Sr_xCuO_4$ sample used in references [12,14]. We obtain $\chi''(\mathbf{Q}_\delta, \omega)$ from the inelastic peak intensity at the incommensurate position $(1 - \delta, \delta, \mathrm{L})$ via

the fluctuation-dissipation theorem and scale our data with a single multiplicative constant to give the best overall agreement. The results are nearly identical within the error bars for these two systems. It appears that the temperature dependence of the spin fluctuations does not depend on the nature of the dopants, Sr^{++} versus O^{--}, with their characteristic quenched versus annealed disorder. Whereas these two samples behave nearly identically, the temperature dependence changes with T_c for the $La_{2-x}Sr_xCuO_4$ system, and, as mentioned above, the optimally doped material exhibits a complete magnetic gap below 3.5 meV while the underdoped materials like those in Figure 5 do not.

It is also instructive to compare the value of the incommensurability δ of the inelastic peaks for La_2CuO_{4+y} with that found for $La_{2-x}Sr_xCuO_4$. In recent work, Yamada *et al.* [19] have found a proportionality between the superconducting transition temperature for highest quality single crystals and δ for samples up to optimal doping. Using the data from Yamada *et al.*, we have constructed a plot, shown in Figure 6, of δ versus T_c that includes our La_2CuO_{4+y} sample which has $T_c = 31$ K and $\delta = 0.105$. It is clear from the figure that the La_2CuO_{4+y} crystal fits perfectly on the straight line defined by the $La_{2-x}Sr_xCuO_4$ samples.

Another important parameter is the width of the inelastic peaks in **q**. Unfortunately, since our La_2CuO_{4+y} samples are still less than one third the volume of the best single crystals of $La_{2-x}Sr_xCuO_4$ that have been studied, the statistics are not as good. Thus we cannot determine the widths with any precision at this time, but it appears that the La_2CuO_{4+y} peaks are broader than those in the $La_{2-x}Sr_xCuO_4$ crystals with similar T_c. We do not believe that this is the result of any anomalous structural disorder; our undoped crystals are state-of-the-art TSFZ grown La_2CuO_4. In addition, as already noted, the oxygen dopants presumably form a more ordered arrangement than do the Sr^{++} dopants. Thus we are led to the speculation that the broad inelastic peaks in La_2CuO_{4+y} could represent the superposition of multiple peaks from layers with different incommensurabilities. This may reflect a staged modulation of excess oxygen as described above. If the oxygen is not uniformly distributed among the layers then one might not expect the doping to be uniform

among the different CuO_2 planes. Accordingly, from the work of Yamada *et al.* one might expect these different doping levels to give different incommensurabilities [19]. Thus the broad peak that we measure may actually represent three separate unresolved peaks with somewhat different **q** positions.

IV. CONCLUSIONS

The most important conclusion of this work is that the existence of incommensurate spin fluctuations in the high temperature superconductors is universal for 214 type systems. The most basic features of the spin fluctuations: their position in reciprocal space and evolution with temperature appear to be independent of the type of dopant, the physical arrangement of the dopants, and the degree of disorder in the crystal. In the oxygen doped 214 crystals the excess oxygen can find its equilibrium arrangement down to temperatures near 200 K. This is well below the relevant magnetic and electronic energies in the problem which are $J \simeq 1500K$ and the band width $W \simeq 2\ J$. This is quite different from the case for Sr^{++} dopants which are in fixed positions at the sample melting temperature near 1400 K. Future experiments on higher stage La_2CuO_{4+y} as well as both underdoped and overdoped $La_{2-x}Sr_xCuO_4$ will serve to elucidate the dependence of the spin excitations and the superconducting magnetic gap on the hole concentration.

V. ACKNOWLEDGEMENTS

We would like to thank F.C. Chou, M. Greven, and J.M. Tranquada for valuable discussions. The work at MIT was supported by the MRSEC Program of the National Science Foundation under award number DMR 94-00334 and by the NSF under award number DMR 93-15715. Research at Brookhaven National Laboratory was carried out under contract No. DE-AC-2-76CH00016, Division of Material Science, U.S. Department of Energy. The work at Tohoku University was supported by a Grant-in-Aid for Scientific Research in Priority

Areas and the U.S.-Japan Collaboration Program on Neutron Scattering sponsored by the Japanese Monbusho.

REFERENCES

[1] B.O. Wells, R.J. Birgeneau, F.C. Chou, Y. Endoh, D.C. Johnston, M.A. Kastner, Y.S.Lee, G. Shirane, J.M. Tranquada, K. Yamada, *Z. Phys.* B **100**, 535 (1996); R.J. Birgeneau, F.C. Chou, Y. Endoh, M.A. Kastner, Y.S. Lee, G. Shirane, J.M. Tranquada, B.O. Wells, K. Yamada, Proceedings of the 10th Anniversary HTS Workshop on Physics, Materials and Applications, Houston, TX (World Scientific, 1996).

[2] B.O. Wells, Y.S. Lee, M.A. Kastner, R.J. Christianson, R.J. Birgeneau, K. Yamada, Y. Endoh, G. Shirane, (unpublished work).

[3] K. Yamada, S. Wakimoto, G. Shirane, C.H. Lee, M.A. Kastner, S. Hosoya, M. Greven, Y. Endoh, R.J. Birgeneau, *Phys. Rev. Lett.* **75**, 1626 (1995) and references therein.

[4] J.D. Jorgensen, B. Dabrowski, S. Pei, D.G. Hink, L. Soderholm, B. Morosin, J.E. Schirber, E.L. Venturini, and D.S. Ginley, *Phys. Rev.* B **38**, 11337 (1994).

[5] D.C. Johnston, F. Borsa, P.C. Canfield, J.H. Cho, F.C. Chou, L.L. Miller, D.R. Torgeson, D. Vaknin, J. Zaretsky, J. Ziolo, J.D. Jorgensen, P.G. Radaelli, A.J. Shultz, J.L. Wagner, S.-W. Cheong, W.R. Bayless, J.E. Schirber, and Z. Fisk, in *Phase Separation in Cuprate Superconductors* ed. Sigmund, E., and Müller, K.A. (Springer-Verlag, Heidelberg, 1994) pp. 82-100.

[6] R.J. Birgeneau and G. Shirane, in *Physical Properties of High Temperature Superconductors*, edited by D.M. Ginsberg (World Scientific, Singapore, 1989), p. 152. A. Aharony, R.J. Birgeneau, A. Coniglio, M.A. Kastner, H.E. Stanley, *Phys. Rev. Lett.* **60**, 1330 (1988).

[7] J.M. Tranquada, Y. Kong, J.E. Lorenzo, D.J. Buttrey, D.E. Rice, V. Sachan, *Phys. Rev.* B **50**, 6340 (1994)

[8] X. Xiong, P. Wochner, S.C. Moss, Y. Cao, K. Koga, M. Fujita, *Phys. Rev. Lett.* **76**, 2997 (1996).

[9] G. Shirane, R.J. Birgeneau, Y. Endoh, and M.A. Kastner, *Physica* B **197**, 158 (1994); R.J. Birgeneau, A. Aharony, N.R. Belk, F.C. Chou, Y. Endoh, M. Greven, S. Hosoya, M.A. Kastner, C.H. Lee, Y.S. Lee, G. Shirane, S. Wakimoto, B.O. Wells, K. Yamada, *J. Phys. Chem. Solids* **56**, 1913 (1995).

[10] T.E. Mason, G. Aeppli, S.M. Hayden, A.P. Ramirez, H.A. Mook, *Phys. Rev. Lett.* **71**, 919 (1993).

[11] M. Greven, R.J. Birgeneau, Y. Endoh, M.A. Kastner, M. Matsuda, and G. Shirane, *Z. Phys.* B **96**, 465 (1995).

[12] M. Matsuda, K. Yamada, Y. Endoh, T.R. Thurston, G. Shirane, R.J. Birgeneau, M.A. Kastner, I. Tanaka, H. Kojima, *Phys. Rev.* B **49**, 6958 (1994).

[13] B. Keimer, N. Belk, R.J. Birgeneau, A. Cassanho, C.Y. Chen, M. Greven, M.A. Kastner, A. Aharony, Y. Endoh, R.W. Erwin, G. Shirane, *Phys. Rev.* B **46**, 14034 (1992).

[14] T.R. Thurston, P.M. Gehring, G. Shirane, R.J. Birgeneau, M.A. Kastner, Y. Endoh, M. Matsuda, K. Yamada, H. Kojima, I.Tanaka, *Phys. Rev.* B **46**, 9128 (1992).

[15] N. Bulut, D. Hone, D.J. Scalapino, N.E. Bickers, *Phys. Rev. Lett.* **64**, 2723 (1990).

[16] Q. Si, Y. Zha, K. Levin, J.P. Lu, *Phys. Rev.* B **47**, 9055 (1993).

[17] T. Tanamoto, H. Kohno, H. Fukuyama, J. Phys. Soc. **63**, 2739 (1994).

[18] S.A. Kivelson and V.J. Emery, Proc. of "Strongly Correlated Electronic Materials: The Los Alamos Symposium 1993," ed. by K.S. Bedell, *et al.* (Addison Wesley, Redwood City, 1994) 619; V.J. Emery and S.A. Kivelson, *Physica* C **235-240**, 189 (1994).

[19] K. Yamada, J. Wada, K. Kurahashi, C.H. Lee, Y. Kimura, S. Wakimoto. Y. Endoh, S. Hosoya, G. Shirane, R.J. Birgeneau, M.A. Kastner, (unpublished).

FIGURES

FIG. 1. Comparison of (a) phase diagram for $La_{2-x}Sr_xCuO_4$ and (b) proposed phase diagram of La_2CuO_{4+y}.

FIG. 2. Position of the inelastic magnetic peaks in reciprocal space. The scan trajectory is given by the arrow.

FIG. 3. Inelastic scans on Sendai-1. The tilt of the scan trajectory is varied from 0° to 3° to 6°, while the temperature and energy transfer are fixed at T = 32 K and E = 2 meV. The lines are fits to the cross-section which includes the $(\frac{1}{2}, \frac{1}{2})$ peak and the four incommensurate peaks, here only the tilt angle is changed.

FIG. 4. Inelastic scans on MIT-1. The tilt of the scan trajectory is fixed at 6°, while the energy transfers and temperatures are varied. The lines are fits to the cross section which includes the four incommensurate peaks only.

FIG. 5. The imaginary part of the susceptibility as a function of temperature for MIT-1 overlayed on data from Ref.[12] for a Sr-doped crystal with similar T_c. A single multiplicative constant is used to scale the data to give the best overall agreement.

FIG. 6. The incommensurablity versus temperature data for $La_{2-x}Sr_xCuO_4$ taken from Yamada *et al.* [19] with the datum point from our La_2CuO_{4+y} crystal MIT-1.

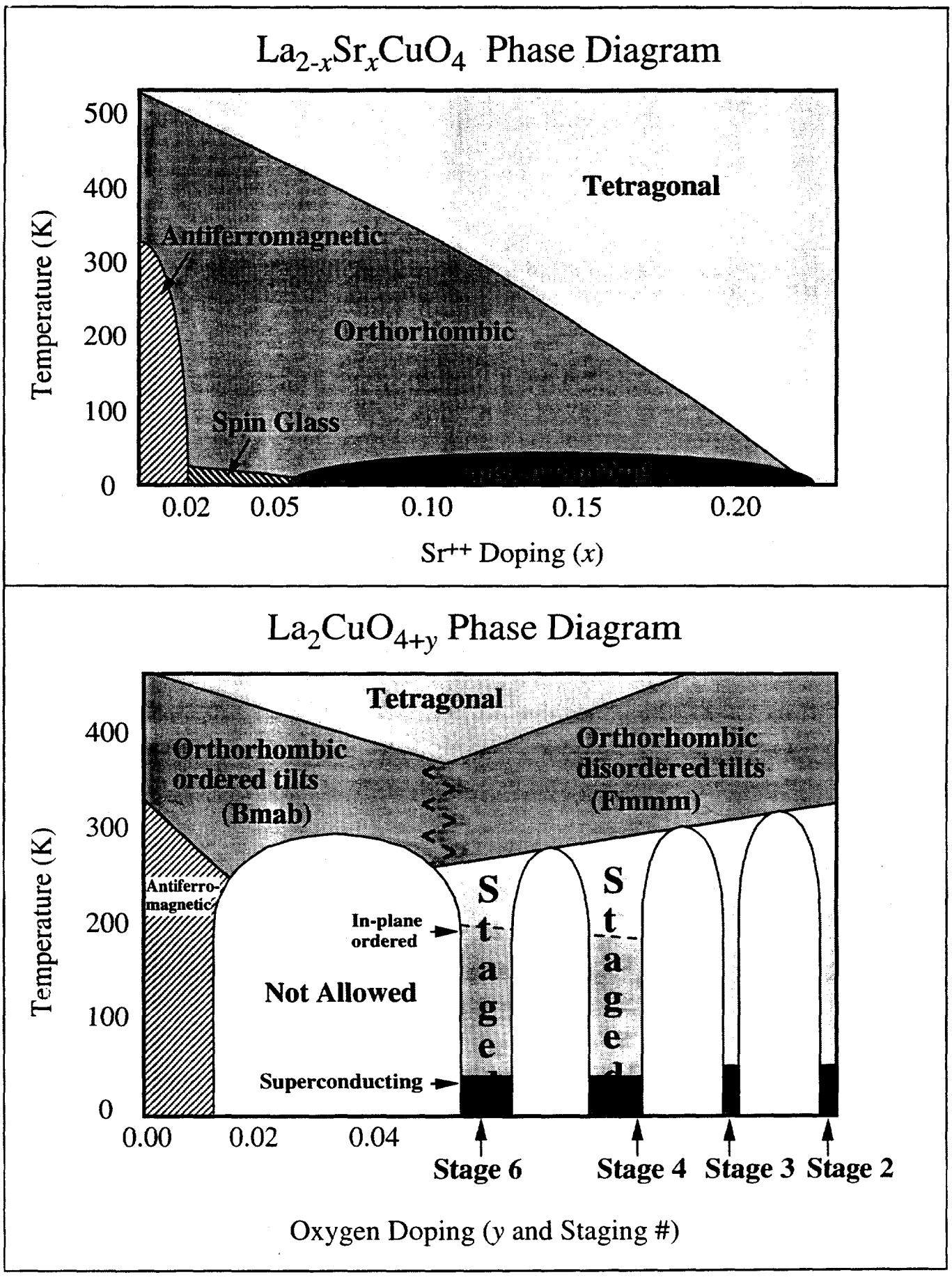
$La_{2-x}Sr_xCuO_4$ Phase Diagram
Temperature (K)
500
400
300
200
100
0
Tetragonal
Antiferromagnetic
Orthorhombic
Spin Glass
0.02
0.05
0.10
0.15
0.20
Sr^{++} Doping (x)
La_2CuO_{4+y} Phase Diagram
Temperature (K)
400
300
200
100
0
Tetragonal
Orthorhombic ordered tilts (Bmab)
Orthorhombic disordered tilts (Fmmm)
Antiferro-magnetic
In-plane ordered
Not Allowed
Superconducting
Stage
Stage
0.00
0.02
0.04
Stage 6
Stage 4
Stage 3
Stage 2
Oxygen Doping (y and Staging #)

Fig. 1

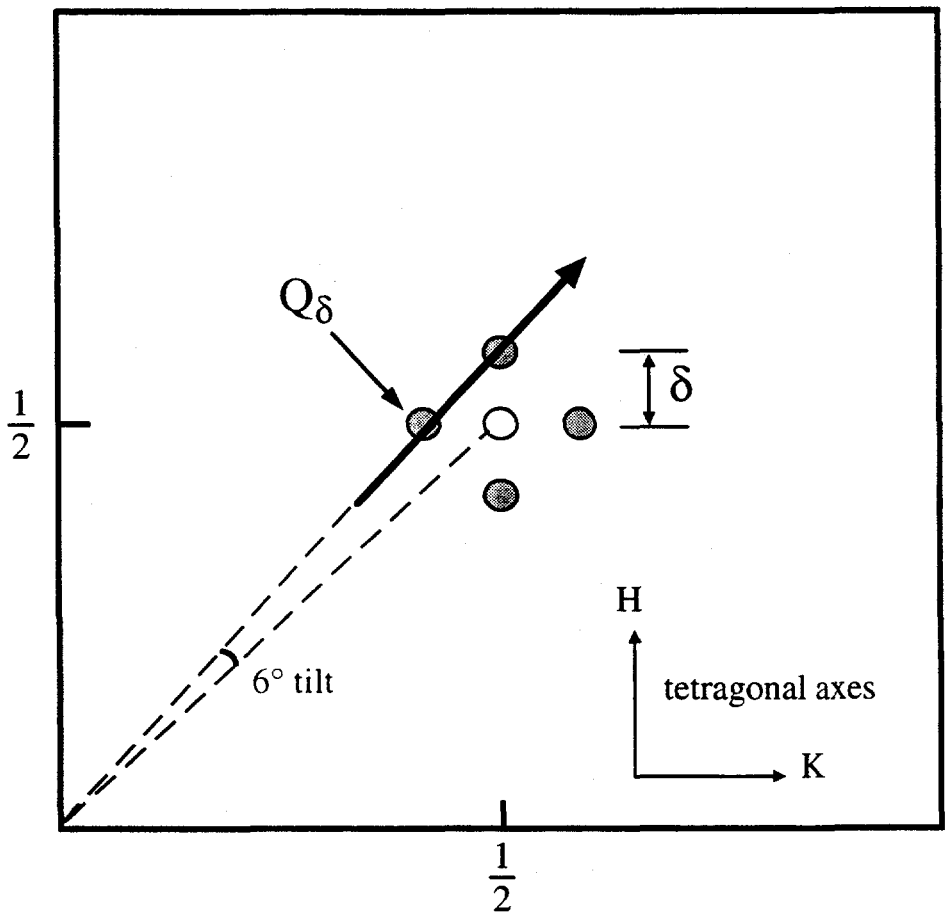

○ (1/2,1/2) peak from undoped portion of crystal

● Incommensurate magnetic peak

⟶ Trajectory of scan

Fig. 2

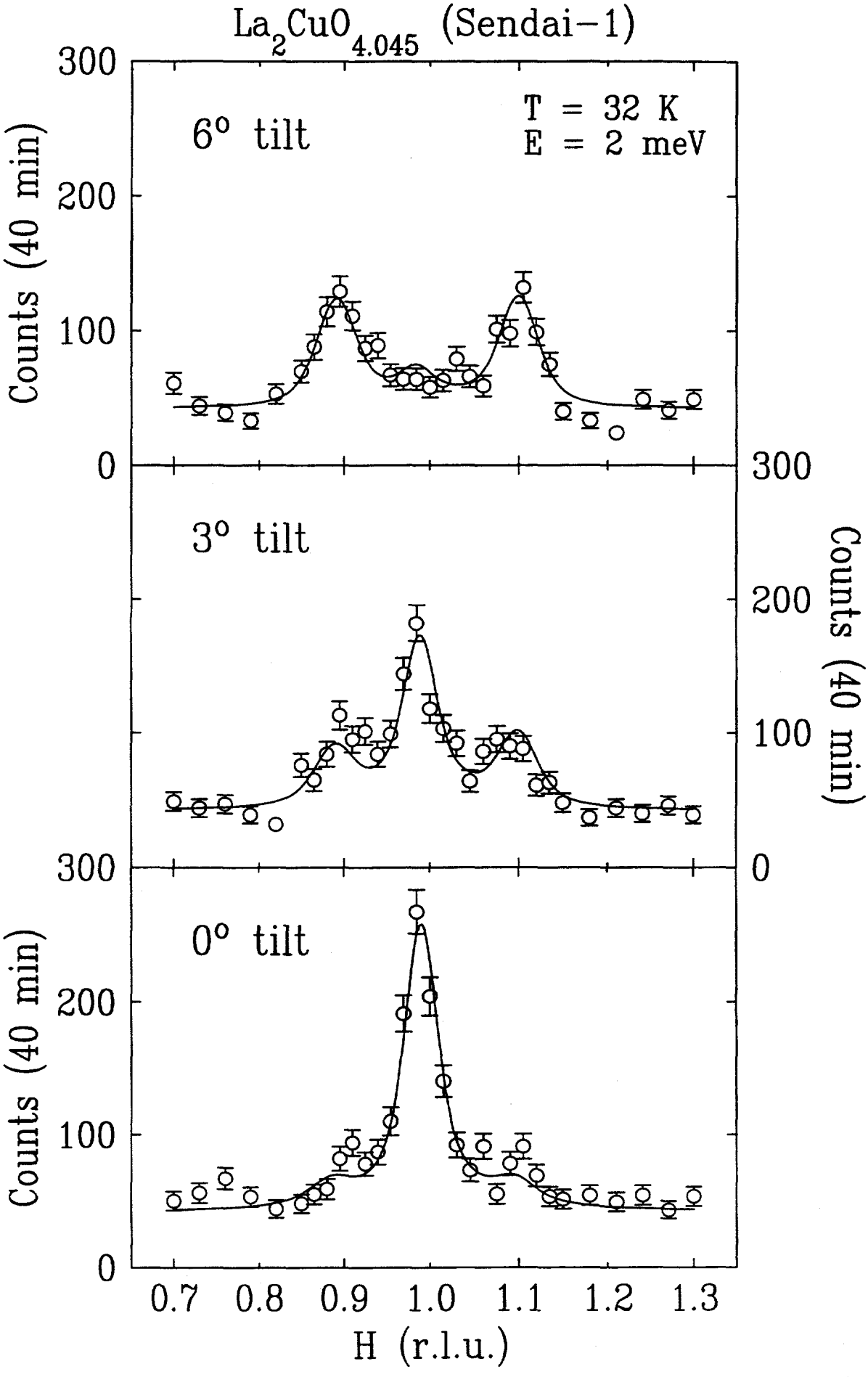
$La_2CuO_{4.045}$ (Sendai-1)
T = 32 K
E = 2 meV
6° tilt
3° tilt
0° tilt
Counts (40 min)
Counts (40 min)
H (r.l.u.)
0
100
200
300
0.7
0.8
0.9
1.0
1.1
1.2
1.3

Fig. 3

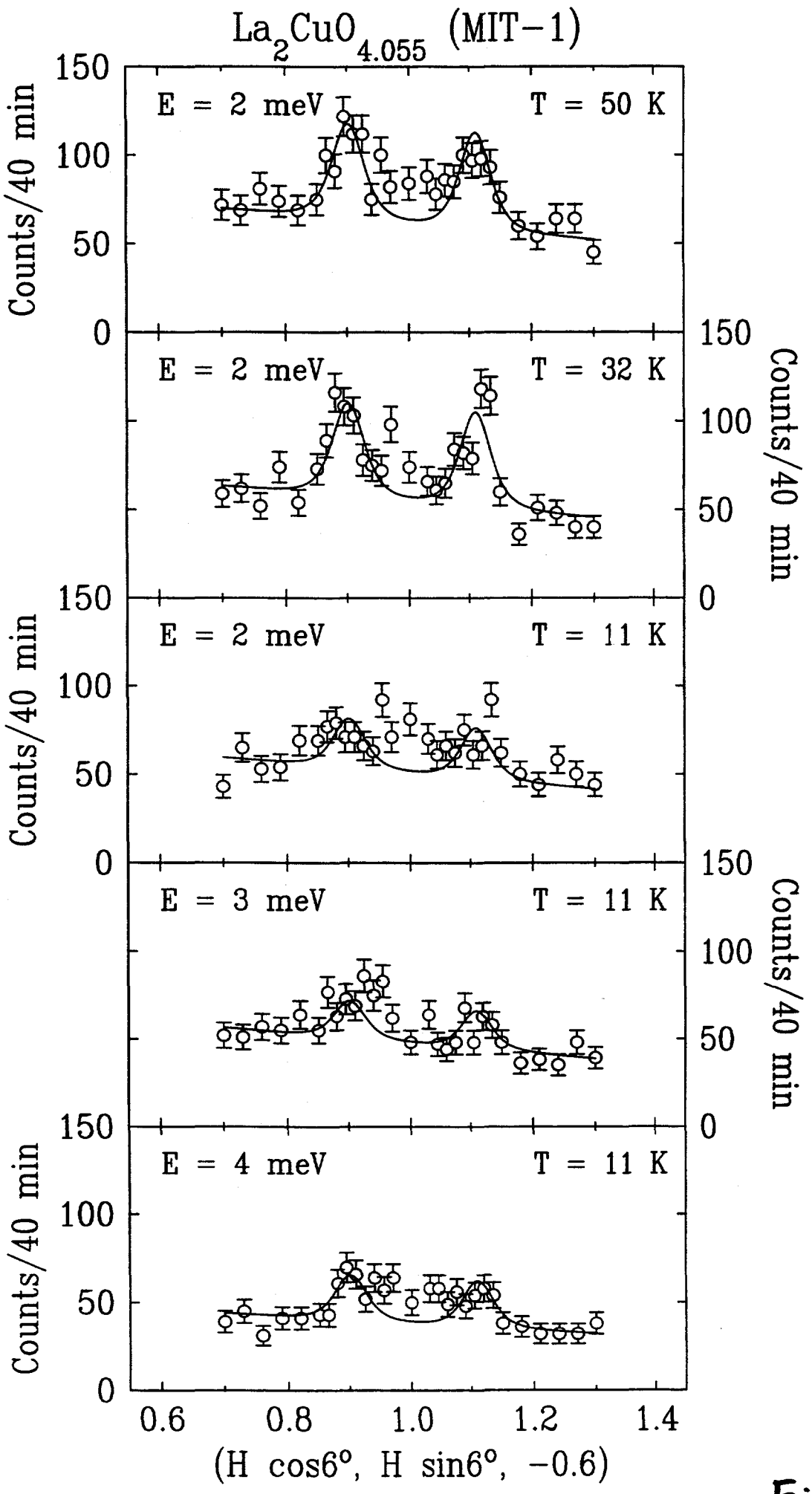
$La_2CuO_{4.055}$ (MIT-1)
E = 2 meV
T = 50 K
E = 2 meV
T = 32 K
E = 2 meV
T = 11 K
E = 3 meV
T = 11 K
E = 4 meV
T = 11 K
Counts/40 min
150
100
50
0
0.6
0.8
1.0
1.2
1.4
(H cos6°, H sin6°, −0.6)

Fig. 4

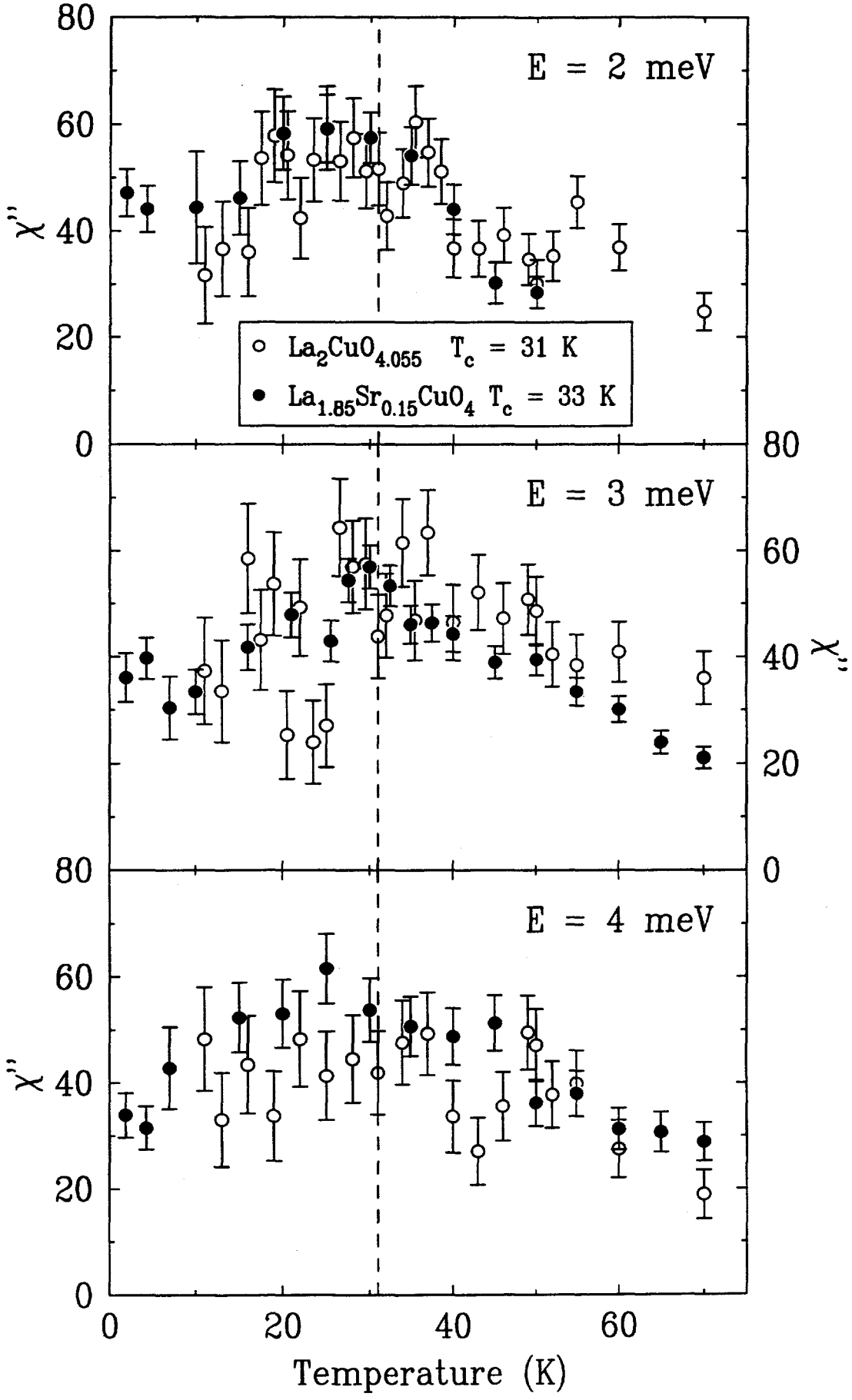
E = 2 meV
E = 3 meV
E = 4 meV
χ''
χ''
χ''
$La_2CuO_{4.055}$ T_c = 31 K
$La_{1.85}Sr_{0.15}CuO_4$ T_c = 33 K
0
20
40
60
80
Temperature (K)

Fig. 5

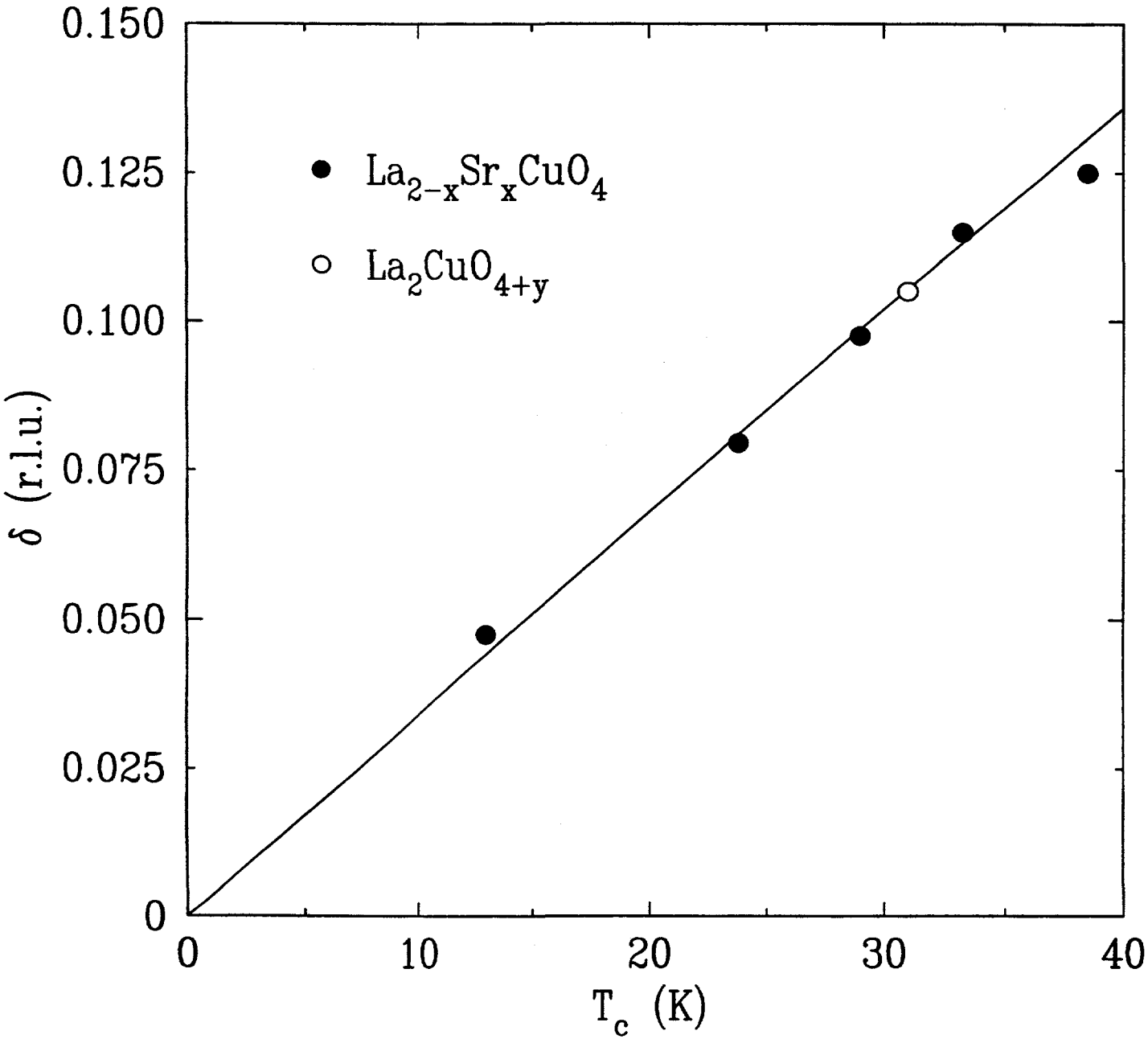
0.150
0.125
0.100
0.075
0.050
0.025
0
δ (r.l.u.)
$La_{2-x}Sr_xCuO_4$
La_2CuO_{4+y}
0
10
20
30
40
T_c (K)

Fig. 6